SAND2016-6009C

Effect of Grid Support Functions and VRT/FRT Capability on Autonomous Anti-Islanding Schemes in Photovoltaic Converters

Michael Ropp[1], Dustin Schultz[1], Jason Neely[2], Sigifredo Gonzalez[2]

[1]Northern Plains Power Technologies (NPPT), Brookings, South Dakota, 57006, USA
[2]Sandia National Laboratories (SNL), Albuquerque, NM, 87123, USA

***Abstract* — The high penetration of utility interconnected photovoltaic systems is is leading to a need for inverters to include grid support functions, to minimize the negative impact these variable distributed energy resources may have on system voltage and frequency. Unfortunately, grid support functions may interfere with island detection algorithms; specifically, it may be difficult for an island detection scheme to detect voltage and frequency deviations if that converter and other converters on the same bus actively modulate their real and reactive power outputs in response to voltage and frequency deviations while also tolerating greater deviation. This report provides analysis and simulation evidence to investigate the effect of advanced inverter functions on the performance of island detection schemes. A mitigation scheme is also presented and shown to be effective in simulation.**

***Keywords* – Distributed Energy Resources, Photovoltaics, Inverters, Islanding, Grid Support Functions**

I. Introduction

Distributed energy resources (DERs) such as photovoltaics (PV) are seeing rapid and widespread deployment on electric power systems (EPSs). When deployment levels become high, it is important that DERs accept some responsibility for maintaining the performance of the grid via so-called "grid support functions" (GSFs) like inertial response, VAr support, and low voltage ride through (LVRT) and low-frequency ride-through (LFRT) [1].

At the same time, since DERs are commonly connected in distribution systems, it remains important that DERs not support the formation of unintentional islands. An island is a section of an EPS that contains its own sources and loads and thus can operate autonomously for at least some period of time. An unintentional island could theoretically form if a DER is energizing a distribution circuit when that circuit becomes isolated from the main grid. Unintentional islands of this type would operate without proper voltage and frequency controls, protection, or visibility to the EPS operator, and can pose risks to equipment or potentially to human safety. Thus, applicable codes and standards require that unintentional islands be prevented.

The worst-case scenario occurs when the local generation and loads are very closely balanced, so that there is essentially no real or reactive power being imported from or exported to the grid. There are many passive and active islanding detection methods [2]-[4] designed to enable detection of this worst case, but most of the best-performing methods in common use today involve manipulating the DER controls so as to destabilize the island. This creates an obvious conflict with GSFs: GSFs act to stabilize and improve grid performance, and islanding detection means act to destabilize and degrade islanded grid performance. Thus, there is some concern that GSF requirements in DERs may lead to degradation of the performance of islanding detection systems.

This paper first presents simulation results on the impact of GSFs on islanding detection, then outlines a method for mitigating that impact by decoupling the performance of islanding detection and GSFs via a "collaborative controls filter" (CCF), and finally presents simulation results on the effectiveness of the CCF. The operation of the CCF relies on temporal separation between the time period over which islanding detection must act (fairly fast) and that over which GSFs need to act (slower). The CCF is described and simulation results illustrating its performance are presented. The results indicate that the CCF works well in the cases tested, enabling robust anti-islanding with GSFs.

II. Collaborative Controls Filter

For this work, we consider a generic converter with volt-VAr and frequency-Watt (FW) functions as well as voltage and frequency ride-through. The converter is configured for an anti-islanding test with an RLC load tuned to provide generation-load balance. A simplified model of this assembly is shown in Figure 1 with the volt-VAr and FW functions shown in the "Advanced Inverter Functions" blocks on the left, the inverter's response approximated by the first-order response blocks in the center, and the load's voltage and frequency response computed by the blocks on the right. Combining the advanced inverter functions shown in Figure 1 with the voltage and frequency response, it can be shown that a closed-loop system can be realized wherein the resulting linearized small-signal response for voltage and frequency is stable. The methodology proposed herein involves the placement of a lag filter before the actuation of FW and volt-VAr functions, allowing the active anti-islanding to disturb the unintended island at high frequencies (>10 Hz) and trigger a disconnect while simultaneously enabling the GSFs to provide adequate support to the grid at lower frequencies. In this way, the CCF "decouples" the GSFs and the islanding detection functions so that the benefits of both can be achieved simultaneously.

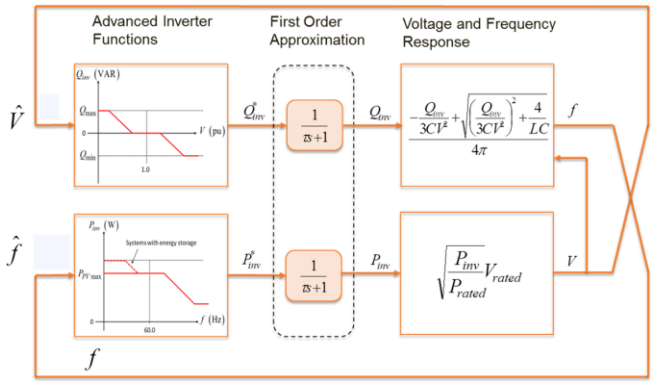

Figure 1: Illustrative reference model showing the role of GSFs in an islanded PV converter.

III. Simulation

This section describes the simulation model used for evaluation and provides simulation results.

A. Simulation Model

The CCF was tested via simulation in MATLAB/SimPowerSystems using the test circuit shown in Figure 2. The test circuit represented in the model is the IEEE 1547 islanding test apparatus and includes a Thevenin-equivalent source at the left, a Yg-Yg distribution transformer with 5.75% impedance, and a tuneable parallel RLC load. To improve realism, R-L circuit impedances are also included, with values derived from the conductor types and lengths used in the islanding test apparatus in the Distributed Energy Technology Laboratory (DETL) at Sandia.

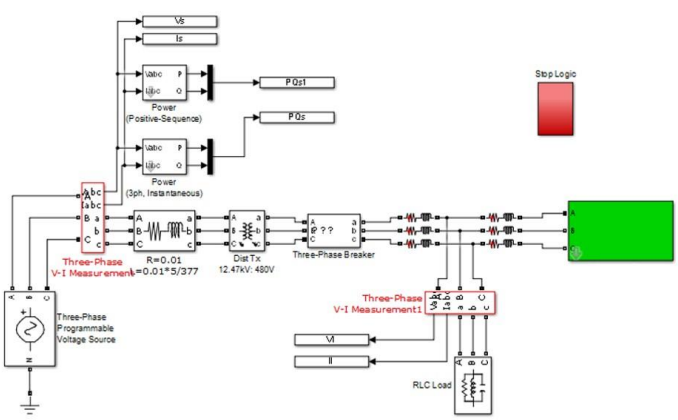

Figure 2. Simulation testbed for testing the CCF.

The green block at the right in Figure 2 contains detailed manufacturer-specific models of two sets of inverters. The first "set" is actually a single inverter, which is a transformer-isolated, single stage, 50 kW three-phase inverter using typical dq0-frame controls. The second set is a set of three single-phase, two-stage, 3 kW inverters connected in grounded-Y. These inverter models were validated using test data obtained in the DETL. The three-phase inverter model matched experimental results very well, and the single-phase inverter models showed reasonable behavioral matching. The islanding detection methods used in the two types of inverter modeled here are fundamentally different:

1. The three-phase inverter utilizes the Sandia Frequency Shift (SFS) method [2] in which the inverter changes its frequency using positive feedback on frequency error and relies on reaching a frequency trip setpoint to cease energizing an unintentional island.
2. The single-phase inverters rely on impedance detection in which changes in voltage corresponding to output current perturbations are measured and the value of $\partial V/\partial I$ gives a measure of the impedance the inverter is looking into [2]. These inverters also incorporate a rate-of-change-of-frequency (RoCoF) relay [2]. Neither of these mechanisms relies on the inverter reaching a frequency trip setpoint.

All four inverters can operate in a standard "IEEE 1547-2003" mode in which the over/under voltage and over/under frequency relays are set according to the values in that standard; or, they can operate in a GSF mode with the following four GSFs:

1. Low-voltage ride-through (also called "fault ride through") in which voltage trips are set as in IEEE 1547A
2. Low-frequency ride-through in which over/under frequency trip settings set as in IEEE 1547A
3. Volt-VAr support via the VV11 curve
4. Frequency-watt support via the FW22 curve

Simulations were run for multiple permutations of irradiance and GSF settings:

- Irradiances of 333, 667, and 1000 W/m^2
- With and without GSFs active
- With and without the CCF

The irradiance was also varied to investigate whether either the impacts of GSFs on anti-islanding, or the effectiveness of the CCF, might be a function of irradiance.

B. Simulation Results

The first set of results is for a "base case" with IEEE 1547-2003 setpoints, no GSFs, and no CCF. The irradiance level was 1 kW/m^2 (inverters at rated power output). Figure 3 shows the base case results via a surface plot of the maximum run-on times (ROTs) versus island real power load and VAr mismatch. Even with the mixture of inverters, the inverter anti-islanding is effective; over the entire range of simulations, the longest ROTs are on the order of 375 ms.

Next, the four GSFs listed above were activated, still under full irradiance. Figure 4 shows a surface plot of ROTs vs. island real power and reactive power mismatch under the same conditions as in Figure 3 except with the GSFs "on".

When the GSFs are turned on, ROTs clearly increase; the maximum ROTs in this case are just under 1000 ms. The GSFs have a clear detrimental impact on the effectiveness of anti-islanding, although it should be noted that in no case did the ROTs become long enough to violate the 2 s maximum ROT allowed by IEEE 1547-2003. Figure 5 is a histogram comparing the results in Figures 3 and 4. The blue bars in Figure 5 are a histogram of the ROTs for the no-GSF case, and the brown bars in Figure 5 represent a histogram of ROTs with the GSFs active, but without the CCF. Figure 5 shows the detrimental impact of the addition of the GSFs on islanding detection effectiveness because the distribution of ROTs shifts significantly to the right.

Next, Figure 6 shows a surface plot of the same situation as in Figure 4, but now with the CCF. Maximum ROTs in Figure 6 are approximately 450 ms. Figure 7 is a histogram in which the blue bars show ROTs with all GSFs on but without the CCF (i.e., the same data as in the orange bars in Figure 5), and the orange bars in Figure 7 are a histogram of ROTs with GSFs and the CCF. Figures 6 and 7 indicate that the negative impact of adding the GSFs has been largely mitigated by adding the CCF; maximum ROTs are approximately 450 ms, and the histogram has shifted back to the left.

Changing the irradiance level had very little impact on the effectiveness of the anti-islanding with GSFs off or on, but it did impact the level of benefit provided by the CCF. Figure 8 shows a surface plot of ROTs under the same conditions as in Figure 3, except that the irradiance as been reduced to 33% (333 W/m^2). Maximum ROTs area approximately 360 ms, nearly the same as those in Figure 3. Figure 9 shows histograms comparing the ROTs with all GSFs on and 1547A trips, with and without the CCF, but at 33% irradiance. The maximum ROTs are approximately the same (~ 1 s) when the GSFs are activated, for both 33% and 100% irradiance. However, the level of benefit obtained from the CCF is lower at 33% irradiance as indicated by the fact that the two distributions in Figure 9 are about the same. The primary culprit in the lengthening of ROTs appears to be the widened trip setpoints and the ride-throughs. However, the island

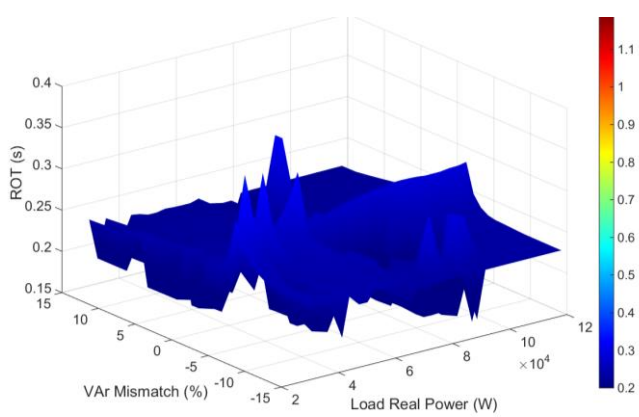

Figure 3. Surface plot of ROTs vs. load real power and island VAr mismatch for 100% irradiance, GSFs "off", and no CCF.

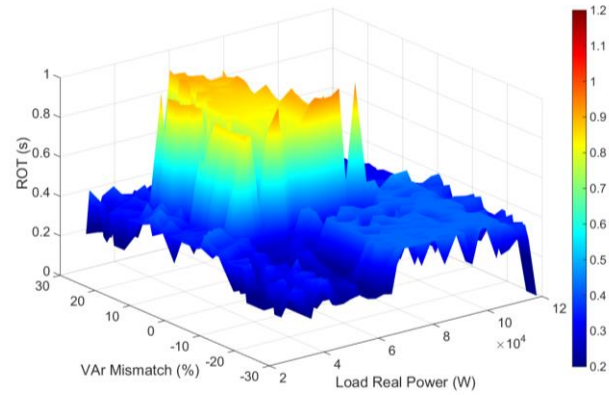

Figure 4. Surface plot of run-on times as a function of load power and VAr mismatch, for 100% irradiance, GSFs "on", and no CCF.

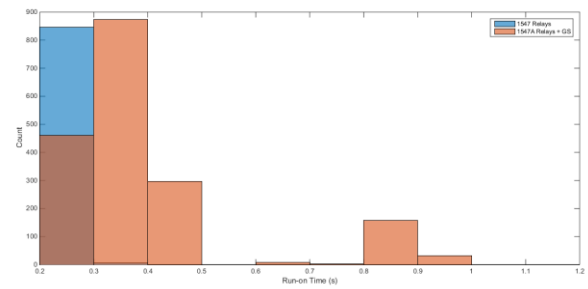

Figure 5. Histograms of ROTs for 100% irradiance and no CCF, without (blue) and with (brown) GSFs.

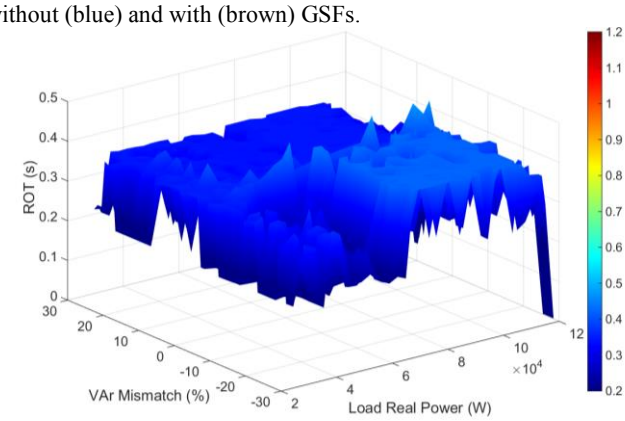

Figure 6. Same conditions as Figure 4, but with the CCF.

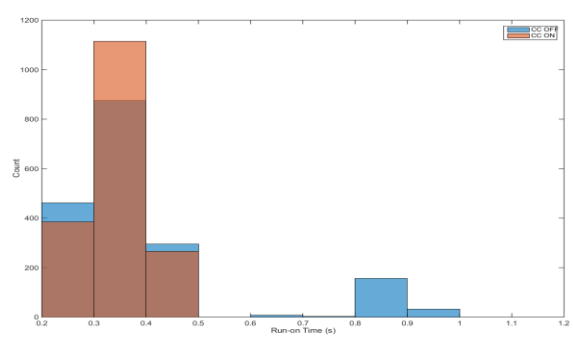

Figure 7. Histogram of ROTs at 100% irradiance with all GSFs active. Blue bars = ROTs with GSFs but no CCF; brown bars = ROTs with GSFs on and with the CCF.

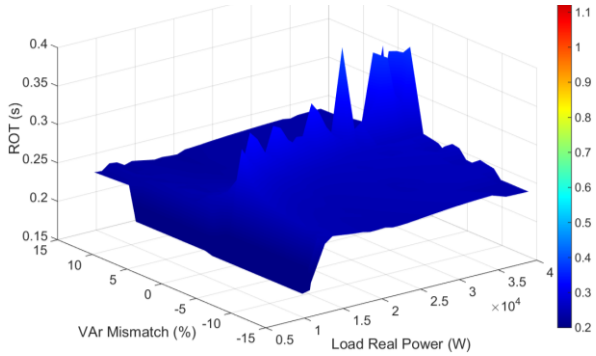

Figure 8. Surface plot of ROTs vs. load real power and island VAr mismatch for 33% irradiance, GSFs "off", and no CCF (i.e., standard island test of the inverter anti-islanding controls).

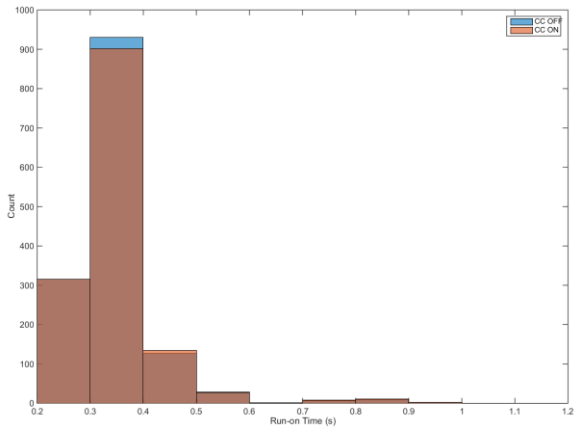

Figure 9. Histogram of ROTs at 33% irradiance with all GSFs active. Blue bars = ROTs with GSFs but no CCF; brown bars = ROTs with GSFs on and with the CCF.

behavior with these inverters was also strongly influenced by the negative sequence behavior of the single-phase inverter set. Figure 10 shows the sequence components of the three phase inverter's output current during an island event with GSFs on, and Figure 11 shows the sequence currents for the three single-phase inverters during the same event. The three-phase inverter maintains a reasonably (but not perfectly) balanced three-phase output, with the imperfection largely stemming from an inability to exactly follow the changing frequency in the island. However, the single phase inverters, once the island is formed, have no controls that maintain 120° separation between the phase currents, and as a result this set of inverters transitions from being a positive sequence current source to a negative sequence current source. The result was that in many tests the inverters actually tripped on overvoltage.

IV. Conclusions

1.) The addition of the GSFs and ride-throughs significantly degraded the effectiveness of the active islanding detection in the inverters, with maximum ROTs increasing by factors of 2 to 3 in all cases. However, in no case did the addition of GSFs or ride-throughs cause ROTs to exceed 2 s.

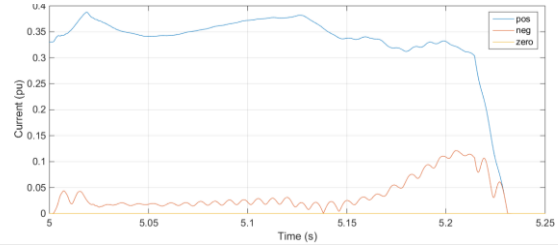

Figure 10. Sequence currents from the three-phase inverter during an island event with GSFs on.

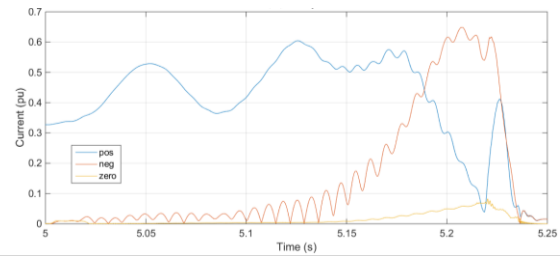

Figure 11. Sequence currents from the set of three single-phase inverters during an island event with GSFs on.

2.) At higher irradiance, the addition of the collaborative controls restored most of the performance of the islanding detection that was lost when the GSFs were activated.

3.) Islanding detection effectiveness did not appear to be a strong function of irradiance level, as long as the inverters were in maximum power point tracking mode (not curtailed).

Acknowledgment

Sandia National Laboratories is a multi-program laboratory managed and operated by Sandia Corporation, a wholly owned subsidiary of Lockheed Martin Corporation, for the U.S. Department of Energy's National Nuclear Security Administration under contract DE-AC04-94AL85000.

References

[1] R. Walling, K. Clark, "Grid Support Functions in Utility-Scale PV Systems", IEEE Transmission and Distribution Conference and Exposition, April 2010, 5 pgs.

[2] W. Bower, M. Ropp, "Evaluation of Islanding Detection Methods for Utility-Interactive Inverters in Photovoltaic Systems; Sandia National Laboratories Technical Report; SAND2002-3591; Albuquerque, NM, November 2002.

[3] F. De Mango, M. Liserre, A. D. Aquila, A. Pigazo, "Overview of Anti-Islanding Algorithms for PV Systems. Part I: Passive Methods," *Power Electronics and Motion Control Conference, 2006. EPE-PEMC 2006. 12th International* , pp.1878,1883, Aug. 30 2006-Sept. 1 2006.

[4] F. De Mango, M. Liserre, A. D. Aquila, "Overview of Anti-Islanding Algorithms for PV Systems. Part II: ActiveMethods,"*Power Electronics and Motion Control Conference, 2006. EPE-PEMC 2006. 12th International*, pp.1884,1889, Aug. 30 2006-Sept. 1 2006.